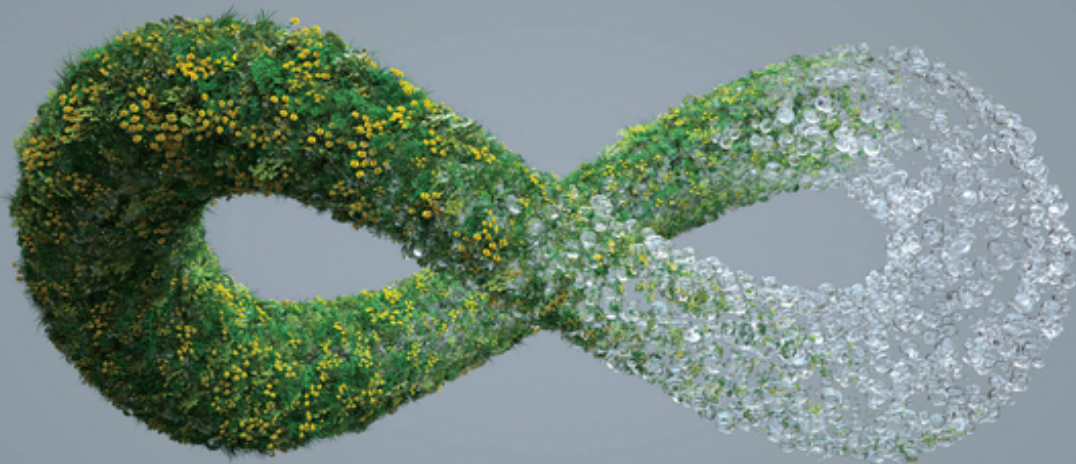


Edited by Shaohua Shen and Shuangyin Wang

Water Photo- and Electro-Catalysis

Mechanisms, Materials, Devices, and Systems



Water Photo- and Electro-Catalysis

Water Photo- and Electro-Catalysis

Mechanisms, Materials, Devices, and Systems

Edited by Shaohua Shen and Shuangyin Wang

WILEY  VCH

Editors**Prof. Shaohua Shen**

Xi'an Jiaotong University
No. 28 Xianning West Street
Xi'an 710049
China

Prof. Shuangyin Wang

Hunan University
No. 2 Lushan Road
Changsha 410082
China

Cover Image: © Andriy Onufriyenko/
Getty Images

■ All books published by **WILEY-VCH** are carefully produced. Nevertheless, authors, editors, and publisher do not warrant the information contained in these books, including this book, to be free of errors. Readers are advised to keep in mind that statements, data, illustrations, procedural details or other items may inadvertently be inaccurate.

Library of Congress Card No.: applied for

British Library Cataloguing-in-Publication Data

A catalogue record for this book is available from the British Library.

**Bibliographic information published by
the Deutsche Nationalbibliothek**

The Deutsche Nationalbibliothek lists this publication in the Deutsche Nationalbibliografie; detailed bibliographic data are available on the Internet at <<http://dnb.d-nb.de>>.

© 2024 WILEY-VCH GmbH, Boschstraße 12,
69469 Weinheim, Germany

All rights reserved (including those of translation into other languages). No part of this book may be reproduced in any form – by photoprinting, microfilm, or any other means – nor transmitted or translated into a machine language without written permission from the publishers. Registered names, trademarks, etc. used in this book, even when not specifically marked as such, are not to be considered unprotected by law.

Print ISBN: 978-3-527-34835-0

ePDF ISBN: 978-3-527-83099-2

ePub ISBN: 978-3-527-83101-2

oBook ISBN: 978-3-527-83100-5

Typesetting: Straive, Chennai, India

Contents

Preface *xiii*

1	Solar Energy Conversion by Dye-sensitized Photocatalysis	1
	<i>Shunta Nishioka and Kazuhiko Maeda</i>	
1.1	Introduction	1
1.2	Light Absorbers	1
1.2.1	Extending the Light Absorption Spectra of Dyes	4
1.2.2	Enhancement of the Absorption Coefficient of Dyes	7
1.2.3	Molecular Design for Efficient Excited-Charge-Carrier Separation and Injection	8
1.2.4	Molecular Design for Facilitating the Regeneration of the Ground State	11
1.2.5	Improving Stability by Forming a Strong Connection Between a Dye and a Semiconductor	12
1.2.6	New Insights Based on the Light Harvesting of a Dye-sensitized Photocatalyst System	13
1.3	Semiconductor Materials	15
1.3.1	Crystallization of a Semicrystalline Semiconductor with Incorporation into Covalent Organic Frameworks	16
1.3.2	Effect of the Number of Active Sites for Photocatalysis	16
1.3.3	Highly Dispersed Active-Site Molybdenum Sulfide Nanoparticles for Proton Reduction Reaction	18
1.3.4	Improving the Solar Energy Conversion Efficiency by Suppressing Undesirable Backward Reactions	19
1.3.5	Immobilization of Dyes on a Reduced Graphene Oxide Surface Through Formation of Chemical Bonds	21
1.3.6	Metal Phospho-Sulfides and -Selenides as Electron-Conducting and Proton-Adsorbing Materials	22
1.3.7	Effects of Dye Adsorption for the Electronic State of the Semiconductor	22
1.4	Dye-sensitized Photocatalysts in Electrochemical Systems	23
1.5	Conclusion	25
	References	27

2	Photocatalytic Hydrogen Production Over CdS-based Photocatalysts	35
	<i>Maochang Liu, Feng Liu, Fei Xue, Jinwen Shi, Hongwen Huang, and Naixu Li</i>	
2.1	Introduction	35
2.2	Basic Principles for Semiconductor-based Photocatalytic H ₂ Production from Water	36
2.3	Chemical Additives for H ₂ Production Enhancement	38
2.4	Construction of CdS-based Heterojunction Photocatalyst to Enhance H ₂ Production	40
2.4.1	Cocatalytic Materials	40
2.4.1.1	Metal Cocatalyst	40
2.4.1.2	Transition-metal Oxides and Hydroxides Cocatalyst	56
2.4.1.3	Transition-metal Sulfide Cocatalyst	60
2.4.1.4	Transition-metal Phosphide and Carbide Cocatalyst	64
2.4.2	Semiconductor–Semiconductor Hetero/homojunction Photocatalyst	67
2.4.2.1	Metal Oxide–CdS Heterojunction Photocatalyst	68
2.4.2.2	Carbon-based Materials–CdS Heterojunction Photocatalyst	71
2.4.2.3	CdS-based Homojunction Photocatalyst	75
2.4.2.4	Metal Sulfide, Selenide–CdS Heterojunction Photocatalyst	78
2.4.2.5	Other Semiconductors–CdS Heterojunction Photocatalyst	83
2.5	Conclusions and Perspectives	86
	References	87
3	Photocatalytic Hydrogen Production System	107
	<i>Yan Yang, Dengwei Jing, Liang Zhao, and Shaohua Shen</i>	
3.1	Introduction	107
3.2	Fundamentals of Hydrogen Production by Photocatalytic Water Splitting	108
3.3	Classifications of the Photocatalytic Hydrogen Production System	109
3.4	Example of Hydrogen Production System by Photocatalytic Water Splitting	111
3.4.1	Introduction of the Pilot Plant	112
3.4.1.1	Solution-Feeding Subsystem	113
3.4.1.2	Photocatalytic Reaction Subsystem	113
3.4.1.3	Gas Collection Subsystem	116
3.4.1.4	Waste Liquid–Discharging Subsystem	116
3.4.2	Operation Strategies of the Pilot Plant	116
3.4.3	Operation Parameters of the Pilot Plant	117
3.4.4	Operation Results of the Pilot Plant	117
3.4.4.1	Experimental Results	117
3.4.4.2	Simulation Results	118
3.4.5	Life Cycle Assessment of the Pilot Plant	123
3.4.5.1	Goal and Scope Definition	124
3.4.5.2	Life Cycle Inventory Analysis	124
3.4.5.3	Life Cycle Assessment Results	127

3.4.5.4	LCA Analysis in Other Regions of China	133
3.5	Future Work in Terms of Challenges and Chances	135
	References	139
4	Photoelectrochemical Water Splitting	143
	<i>Jinzhan Su and Zhiqiang Wang</i>	
4.1	Introduction	143
4.2	Oxide Semiconductor	144
4.3	Sulfide Semiconductor	150
4.3.1	CdS	150
4.3.2	CdSe	151
4.3.3	CdTe	153
4.3.4	CuInS ₂	154
4.3.5	CuGaSe ₂	156
4.3.6	Sb ₂ Se ₃	157
4.4	Silicon and III-V Group GaAs, GaN, GaInAs/GaInP/AlInP	159
4.5	Nitride and Oxynitride Semiconductor	165
4.5.1	C ₃ N ₄	166
4.5.2	Ta ₃ N ₅	166
4.5.3	GaN, InN	169
4.5.4	TiN, Co ₃ N, etc.	170
4.5.5	TaON	170
4.5.6	GaON, LaTiO ₂ N, etc.	172
4.6	Dye-sensitized Photocatalysts	172
4.7	Strategies for Improving PEC Performance	174
4.7.1	Nanostructure	174
4.7.2	Heterojunction	176
4.7.3	Light Absorption	178
4.7.4	Charge Carrier Separation	180
4.7.5	Oxygen Evolution Cocatalysts	181
4.7.6	Surface Protection Layer	183
4.7.7	Surface Passivation Layer	184
4.8	Summary	186
	References	187
5	Photoelectrochemical and Photovoltaic-Electrochemical Water Splitting	207
	<i>Qingjie Wang, Jia Zhao, and Jingshan Luo</i>	
5.1	Introduction	207
5.2	PEC Water Splitting: Theory and Working Principles	209
5.3	Photoanodes	210
5.3.1	TiO ₂ Photoanode	210
5.3.2	Silicon (Si) Photoanode	213
5.3.3	BiVO ₄ Photoanode	214
5.3.4	Fe ₂ O ₃ Photoanode	216

5.4	Photocathodes	218
5.4.1	Cu ₂ O Photocathode	218
5.4.2	Si Photocathode	220
5.4.3	Sb ₂ Se ₃ Photocathode	220
5.5	Tandem Devices	222
5.6	PV-EC Water Splitting	224
5.6.1	Si-based PV-EC System	225
5.6.2	III-V Solar Cell-based PV-EC System	226
5.6.3	Perovskite Solar Cell-based PV-EC System	227
5.6.4	Organic Solar Cell-based PV-EC System	229
5.6.5	CuIn _x Ga _{1-x} Se ₂ Solar Cell-based PV-EC System	232
5.6.6	Dye-sensitized Solar Cell-based PV-EC System	232
5.7	Conclusion	233
	Acknowledgments	233
	References	234
6	Electrocatalytic Reduction of Carbon Dioxide	241
	<i>Kejun Chen, Hongmei Li, Junwei Fu, Xiqing Wang, and Min Liu</i>	
6.1	Introduction	241
6.2	Fundamentals of Electrocatalytic Reduction of CO ₂	242
6.2.1	Reaction Pathways and Mechanism	242
6.2.2	Crucial Parameters for CO ₂ Electroreduction Measurements	244
6.3	Electrolytes	246
6.3.1	Aqueous Electrolytes	247
6.3.1.1	Effect of the Electrolyte pH	247
6.3.1.2	Cation Effects	248
6.3.1.3	Anion Effects	249
6.3.2	Nonaqueous Electrolyte	249
6.3.3	Ionic Liquids	250
6.4	Catalysts for Electrochemical CO ₂ Reduction	250
6.4.1	Metal Catalysts	250
6.4.1.1	Metal Catalysts for Reduction of CO ₂ into Formate	251
6.4.1.2	Metal Catalysts for Reduction of CO ₂ into CO	252
6.4.1.3	Metal Catalysts for Reduction of CO ₂ into Hydrocarbons and Alcohols	253
6.4.2	Single-atom/Site Catalysts for Electrochemical Reduction of CO ₂	253
6.4.2.1	Fe-based Single-atom/Site Electrocatalysts	253
6.4.2.2	Co-based Single-atom/Site Electrocatalysts	254
6.4.2.3	Ni-based Single-atom/Site Electrocatalysts	256
6.4.2.4	Cu-based Single-atom/Site Electrocatalysts	256
6.4.2.5	Sn-based Single-atom Electrocatalysts	256
6.4.2.6	Other Metal-based Single-atom Electrocatalysts	257
6.4.2.7	Single-atom Alloy Electrocatalysts	257
6.5	Gas Diffusion Electrode for E-CO ₂ RR	259
6.5.1	Gas Diffusion Layer	260

6.5.2	Catalyst Layer	261
6.5.3	Flow Cell	262
6.5.4	Membrane Electrode Assembly (MEA) Cell	264
6.6	Summary and Outlook	265
	References	266
7	Electrocatalytic Nitrogen Reduction with Water	273
	<i>Chen Chen and Shuangyin Wang</i>	
7.1	The Design and Regulation Strategy of Nitrogen Reduction Reaction (NRR) Catalysts	273
7.1.1	Defect Engineering	273
7.1.1.1	Doping Defect	273
7.1.1.2	Atom Vacancy	277
7.1.2	Atom Engineering	279
7.1.2.1	Single/Double-atoms Catalysis	279
7.1.2.2	Enzyme-like Catalysis	280
7.2	The Influence of Reaction Microenvironment	281
7.2.1	The Effect of Electrolyte Solution	281
7.2.1.1	pH Effect	282
7.2.1.2	Ionic Effect	283
7.2.1.3	Molecular Crowding Effect	284
7.2.2	The Effect of Catalyst Surface Environment	285
7.3	In Situ Characterization Method and Mechanism of Nitrogen Reduction	286
7.3.1	NRR Mechanism	286
7.3.2	In Situ Electrochemical Characterizations for Active Species	289
7.3.2.1	In Situ Fourier-transformed Infrared Spectroscopy (FTIR) Measurement	289
7.3.2.2	In Situ Differential Electrochemical Mass Spectrometry (DEMS) Measurement	289
7.3.2.3	In Situ Scanning Tunneling Microscopy (EC-STM)	292
7.3.2.4	In Situ X-ray Absorption Spectroscopy (XAS) and In Situ Raman Measurement	292
7.3.3	Detection Method for the Nitrogen Reduction Reaction	295
7.3.3.1	Ammonia Detection	296
7.3.3.2	NO _x Contaminations	297
7.3.3.3	Rigorous Experimental Protocols for ENR	298
	References	300
8	Recent Advances in Electrocatalytic Organic Transformations Coupled with H₂ Evolution	303
	<i>Xiao Shang, Jian-Hong Tang, and Yujie Sun</i>	
8.1	Introduction	303
8.2	Representative Organic Compounds for Anodic Oxidation	305
8.2.1	Oxidation of Hydrocarbons	305

8.2.2	Oxidation of Oxygen-containing Compounds	307
8.2.3	Oxidation of Amines	309
8.3	Representative Anodic Addition Reactions with Nucleophiles and Radicals	310
8.3.1	Cyanation Reactions	310
8.3.2	Trifluoromethylation Reactions	310
8.3.3	Halogenation Reactions	311
8.4	Oxidative Coupling Reactions Coupled with H ₂ Production	312
8.4.1	C–C Coupling Reactions	312
8.4.2	C–N Coupling Reactions	312
8.4.3	C–O Oxygenation Reactions	314
8.4.4	C–S Coupling Reactions	315
8.4.5	C–P Coupling Reactions	316
8.4.6	S–S Coupling Reactions	317
8.5	Conclusions	317
	Acknowledgments	317
	References	318

9 The Advancement of Catalysts for Proton-Exchange Membrane Fuel Cells 321

Yi Cheng and Shuangyin Wang

9.1	The Introduction of Proton-Exchange Membrane Fuel Cells	321
9.2	Proton-Exchange Membrane Fuel Cells	323
9.3	The Anode Hydrogen Oxidation Reaction	324
9.3.1	Hydrogen Oxidation Reaction Mechanism	324
9.4	The Cathode Oxygen Reduction Reaction	326
9.4.1	ORR Mechanism	326
9.4.2	Platinum-group-metal-based Catalysts	328
9.4.2.1	Size Control – from Nanoparticle to Single Atoms	328
9.4.2.2	Composition Control	331
9.4.2.3	Shape Engineering	334
9.4.2.4	Atomic Ordering	338
9.4.3	PGM-free Catalysts	341
9.4.3.1	One-pot Pyrolysis	343
9.4.3.2	Template-derived Structures	343
9.4.3.3	MOF-derived Structures	345
9.5	Conclusions and Remarks	347
	References	348

10 Advanced X-ray Absorption Spectroscopy on Electrocatalysts and Photocatalysts 363

Kumaravelu Thanigai Arul, Ta Thi Thuy Nga, Chung-Li Dong, and Wu-Ching Chou

10.1	Introduction	363
10.2	Synchrotron-based X-ray Absorption Spectroscopy	364

10.2.1	Progress of In Situ Cells	366
10.3	Energy Generation Systems	368
10.3.1	Electrocatalysts	369
10.3.2	Photocatalysts	375
10.3.3	Photoelectrocatalysts	383
10.4	Summary and Future Outlook	386
	Acknowledgments	388
	References	388
11	Advanced <i>Operando</i>/In Situ Spectroscopy Studies on Photocatalysis for Solar Water Splitting	397
	<i>Dongfeng Li, Fengtao Fan, Can Li, and Xiuli Wang</i>	
11.1	Introduction	397
11.2	Basic Principles of Electromagnetic Spectrum	398
11.3	Pump-Probe Principle for Spectroscopy Techniques	399
11.4	Basic Photophysical Processes in Photocatalysts	400
11.5	Photochemical and Photocatalytic Processes	406
11.5.1	Electron Transition in the Outer Shell	407
11.5.1.1	Transient Absorption/Diffuse Reflectance Spectroscopy (TAS/TDRS)	408
11.5.1.2	Photoinduced Absorption Spectroscopy (PIAS)	412
11.5.1.3	Spectroelectrochemical Absorption Spectroscopy (SECAS)	416
11.5.1.4	Photoluminescence (PL) Spectroscopy and Time-resolved Photoluminescence (TRPL) Spectroscopy	420
11.5.2	Vibrational Transition of Outer Shell	424
11.5.2.1	Infrared (IR) Spectroscopy	425
11.5.2.2	Raman Spectroscopy	428
11.5.3	Electron Transition of Inner Shell	431
11.5.4	Other Developing <i>Operando</i> /In Situ Spectroscopy Techniques	438
11.6	Summary and Future Prospects	439
	References	440
	Index	449

Preface

I believe that water will one day be employed as a fuel, that hydrogen and oxygen that constitute it, used singly or together, will furnish an inexhaustible source of heat and light, of an intensity of which coal is not capable.

—Jules Verne

Water, consisting of hydrogen and oxygen, could act as a sustainable reactant or product to participate in various chemical reactions along with clean energy conversion. As driven by solar energy or thus-generated electricity, water photo- and electro-catalysis for hydrogen evolution reaction (HER) and oxygen evolution reaction (OER) has been considered as an effective approach to green hydrogen production. In reverse electrocatalysis processes, hydrogen oxidation reaction (HOR) and oxygen reduction reaction (ORR) inevitably happen in a fuel cell, which has been considered as a promising technology for green electricity generation. It should be further noted that, by acting as the reactant for electrocatalysis, water could drive the reactions of CO_2 (CO_2RR) and N_2 (NRR) reduction to produce value-added chemicals and fuels (e.g. hydrocarbons and NH_3), and even realize organic transformations coupled with H_2 production. Thus, water photo- and electro-catalysis is becoming an increasingly important field while being considered as an important way to solve the global problems of energy shortage and environmental pollution, and is indeed the technology of the twenty-first century by significantly impacting on human activity,

This book aims to bring together the latest developments in water photo- and electro-catalysis with a focus on its impact on the energy agenda, which splits broadly into different technologies including photocatalysis, photoelectrocatalysis, electrocatalysis, and photovoltaic-electrocatalysis for HER, OER, HOR, ORR, CO_2RR , NRR , and organic transformations. This book shows how the underlying principles are being used across these fields to develop technology with improved functionality and high operating efficiency in terms of water-involved energy conversion reactions. It consists of 11 chapters and introduces different technologies of water photo- and electro-catalysis for energy conversion. The basic mechanisms, emerging materials, devices, and systems of water photo- and electro-catalysis for energy conversion are intrinsically linked, by covering: (i) the fundamentals, materials, and systems of semiconductor-based photocatalytic water

splitting; (ii) the mechanisms, photoelectrode/catalyst materials, and devices of photoelectrocatalytic and photovoltaic-electrocatalytic water splitting; (iii) the fundamentals, materials, and devices for water electrocatalysis, including HER, OER, HOR, and ORR; (iv) the materials and devices for electrocatalytic CO₂RR, NRR, and organic transformations; (v) the advanced characterizations on water photo- and electro-catalysis.

In the past years, exciting breakthroughs in materials and nanotechnology have stimulated a huge amount of renewed interest in this field, although some critical issues of materials, like poor sunlight absorption, poor electric conductivity, and retarded water electrocatalysis kinetics, have thwarted many earlier efforts to reach the “Holy Grail” of photo- and electro-catalysis for energy conversion with economic and ecological sustainability. While we cannot even hope to approach completeness of such technologies in a single book, we nevertheless hope that both scientists and engineers, experts and newcomers in this field find some useful information and details here those can help their academic research and industrial development.

We would like to appreciate the efforts from all the contributors and also the financial support from the National Natural Science Foundation of China (52225606, 51888103).

3 August 2023
Xi'an, China

Shaohua Shen, PhD
Xi'an Jiaotong University, China

Shuangyin Wang, PhD
Hunan University, China

1

Solar Energy Conversion by Dye-sensitized Photocatalysis

Shunta Nishioka and Kazuhiko Maeda

School of Science, Tokyo Institute of Technology, Department of Chemistry, Tokyo 152-8550, Japan

1.1 Introduction

Dye sensitization enables the generation of charge carriers in a wide-bandgap semiconductor under irradiation by visible light that cannot be absorbed by the semiconductor. Dye-sensitized photocatalysis (DSP) was first proposed by Gerischer in 1972 [1] and was later demonstrated by Grätzel et al. [2]. Because of its potential applications in solar energy conversion, DSP has been studied for decades, especially for H_2 evolution via water splitting [3–5]. The DSP H_2 -evolution system consists of two building blocks—a light absorber and a semiconductor material (Figure 1.1)—and the H_2 evolution reaction proceeds as follows: First, the photosensitizer absorbs light and is excited (1). The excited dye injects an electron into a semiconductor (2). The injected electron is consumed via a proton-reduction reaction on the semiconductor’s surface, and H_2 is evolved (3). The oxidized light absorber generated by the electron injection returns to the ground state by accepting an electron from a reductant (4). Unfortunately, some undesirable reactions can occur during this reaction scheme (5–7). To improve the overall efficiency of this system, researchers have devoted extensive effort to promoting the forward reactions and impeding the backward reactions.

In this chapter, we present the strategies for improving DSP systems by separating each building block, pointing out the important factors that influence the DSP performance. We survey recent achievements in the DSP field, especially those related to water-splitting systems, including electrochemical systems, and discuss how various factors can be controlled to improve the performance of dye-sensitized systems.

1.2 Light Absorbers

The development of photosensitizers has been rapidly promoted with the growth of the dye-sensitized solar cell (DSSC) field, which has been pioneered by

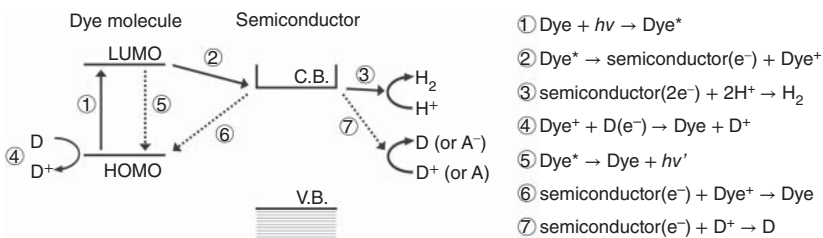


Figure 1.1 Electron transfer processes in a dye-sensitized photocatalysis system. C.B., conduction band; V.B., valence band; HOMO, highest occupied molecular orbital; LUMO, lowest unoccupied molecular orbital; D, electron donor; D⁺: oxidized electron donor; A, electron acceptor; A⁻, reduced electron acceptor. Solid and broken arrows represent forward and backward electron transfers, respectively.

Tsubomura and coworkers [6] and by O'Regan and Grätzel [7]. The practical application of dye-sensitized photovoltaic cells became realistic with the development of a trinuclear Ru complex that possesses two cyano-bridges and four carboxyl-anchoring groups (Figure 1.2a) [8]. A substantial achievement in the DSSC field is the exploitation of the **N3** dye (Figure 1.2b); the electron-injection quantum yield (QY) from **N3** into TiO₂ has reached almost unity, with a solar-to-electric conversion efficiency of 10% under AM1.5G illumination [9]. The structure of **N3** is very similar to the anchoring unit of the trinuclear dye in that **N3** has four carboxyl-anchoring moieties and two isothiocyanato ligands. The next excellent dye developed was **N719** (Figure 1.2c), which gave a power conversion efficiency greater than 9.18% under AM1.5G. This value is still high even now, although the original work was published 20 years ago [10, 11]. These highly efficient dyes for DSSCs, however, have not been well utilized in DSP systems because of the difference in the DSSC and DSP catalytic cycles. In the case of DSSCs, the injected electrons in a semiconductor (e.g. TiO₂) should migrate quickly to reach the counter electrode through an external circuit. Because of the rapid collection of the injected electrons, acceleration of the electron-injection process by strong coupling between the dye and the semiconductor is effective for DSSC systems. In the case of DSP, however, a surface catalytic reaction involving multi-electron transfer (e.g. proton reduction) would become the rate-determining step, whose time scale is at least four orders of magnitude slower than that of the excited-charge-carrier transfer processes [5]. This is distinct from DSSCs, which are operated by single electron transfer processes. Accelerating the electron injection leads to an increase in the standby electrons in the conduction band for the catalytic reaction, which is not effective for DSP systems. On the contrary, the strong coupling may promote undesirable back electron transfer from the conductive substrate to the oxidized dye [12]. Therefore, the dyes developed for DSSCs need to be modified for use in DSP systems. In this section, new dyes developed for efficient DSSCs are introduced and then dye sensitizers optimized for DSP are discussed.

Before moving to the details, we here explain the basic molecular design of photosensitizers. One of the most studied classes of dyes is metal complexes, which have been used in pioneering research in DSP systems [2, 3, 5] and DSSCs

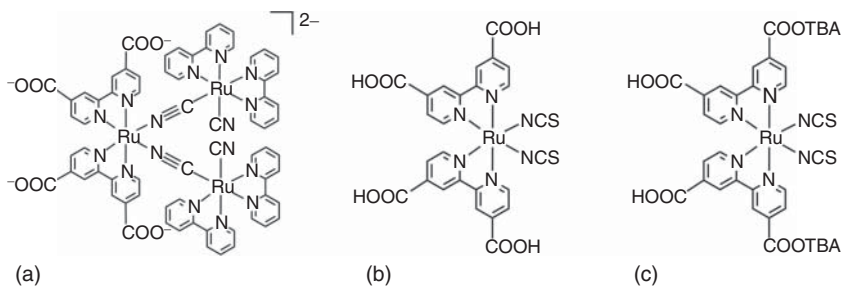


Figure 1.2 Molecular structures of (a) $[\text{Ru}(\text{bpy})_2(\text{CN})_2]_2\text{Ru}(\text{bpy}(\text{COO})_2)_2^{2-}$ ($\text{bpy} = 2,2'$ -bipyridine), (b) **N3**, and (c) **N719**. TBA: tetrabutylammonium.

[4, 7–11]. Recent advances in the DSP for H_2 evolution have included the development of Ru [13], Zn [14], and Ir [15] complexes, and these complexes are still mainstream materials used in the DSP field because their photo- and physico-chemical properties are chemically controllable. Visible-light absorption by metal complexes used in dye-sensitized systems originates mainly from metal-to-ligand charge transfer (MLCT). The highest occupied molecular orbital (HOMO) and the lowest unoccupied molecular orbital (LUMO) are distributed around the metal center and the ligands, respectively. There are three important properties for an effective sensitizer: (i) wide and strong absorption in the visible region, (ii) an efficient excited-charge-carrier transfer cycle, and (iii) high stability. Shifting the HOMO and LUMO levels varies the light-absorption properties of dyes. Efficient excited-charge-carrier transfer is achieved through vectorial electron transfer. Increased stability is attained via strong adsorption onto a semiconductor.

All three of the aforementioned important properties for designed dye molecules can be achieved through adaptation of the ligands of the metal complex. A tris(bipyridine)ruthenium(II) derivative is a good example for explaining the molecular design of metal complexes (Figure 1.3a). For a dye to adsorb onto a semiconductor, at least one of the bipyridine ligands should be functionalized with an anchoring moiety, which should be located at the position closest to the semiconductor substrate. In such a case, the LUMO of the complex is distributed at the functionalized bipyridine ligand, which enhances electron injection from the excited-state complex into the semiconductor. Therefore, if the other peripheral ligand(s) possess a higher energy than the anchoring ligand, the excited electrons would gather on the anchoring ligand, thereby accelerating the electron injection. In addition, because the electron density of the metal center should be increased to ensure wide visible-light absorption, the peripheral ligand(s) should demonstrate electron-donating behavior. Triphenylamine, which exhibits strong electron-donating ability, was introduced onto a Ru complex as a secondary electron donor unit [16]. Although a triphenylamine-based dye had been studied previously [17], excellent dyes that possess a triphenylamine moiety as an electron donor were developed in the same period [18–20]. The triphenylamine-based dyes have a donor- π -acceptor (D- π -A) conjugated structure, which consists of carbon–carbon double-bonded π -bridges and a cyano electron-acceptor group

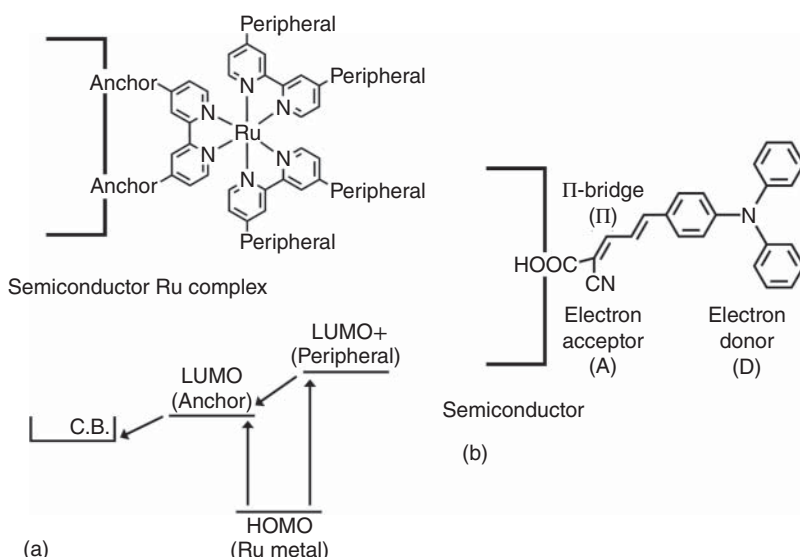


Figure 1.3 Structures of (a) a Ru trisdiimine complex and (b) a triphenylamine-based organic sensitizer. The bottom of figure (a) shows a schematic of the electron-transfer processes of a Ru complex–semiconductor hybrid material. LUMO+: an unoccupied molecular orbital with an energy level higher than that of the LUMO.

(Figure 1.3b). The D- π -A structure enables vectorial charge transfer, which is one of the aforementioned important characteristics of dye-sensitized systems. One of the triphenylamine-based dyes gave an overall **DSSC** efficiency of 5.3%, which is similar to the efficiency of N719 (7.7%). This advancement triggered the rapid development of organic dyes, which are now also used for DSP H₂ evolution. DSP for H₂ evolution has been studied using triphenylamine [21, 22], an organoboron complex [23], coumarin [24], perylene [25], calixarene [26], and tetrathiafulvalene [27], as building blocks for photosensitizers. During the development of these photosensitizers, numerous factors for improving dye-sensitized systems have been revealed. We here discuss these factors, along with some examples of dyes demonstrating the effect of each factor.

1.2.1 Extending the Light Absorption Spectra of Dyes

Extending the absorption spectrum of a dye is a common approach to efficiently utilizing sunlight for solar energy conversion. The strategy for extending the absorption of a dye appears simple: shift the LUMO downward and/or the HOMO upward. The reality, however, is not straightforward because two requirements must be met [28]. First, an excited-state dye must inject an electron into the semiconductor. Second, a sensitizer needs to oxidize a reductant or electron mediator to regenerate the ground state. Extensive efforts have been devoted to developing new photosensitizers that enable the more efficient utilization of solar energy while still achieving these two requirements.

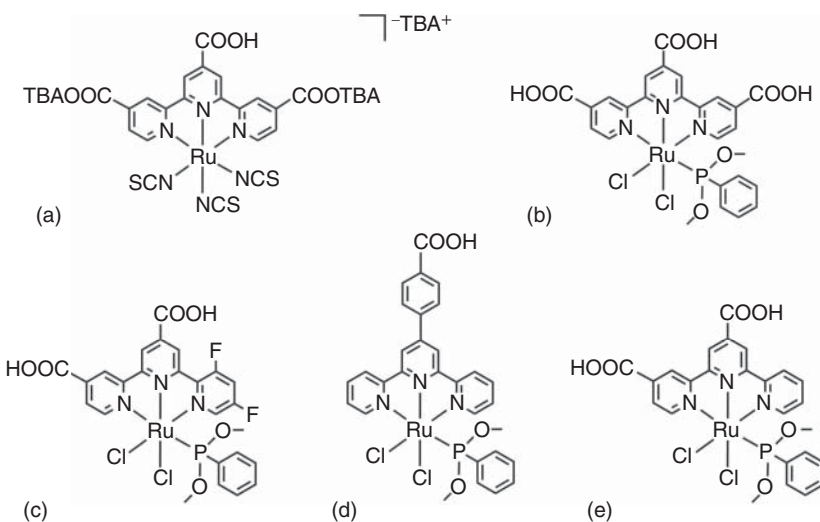


Figure 1.4 Molecular structures of the (a) **N749**, (b) **DX1**, (c) **GS11**, (d) **GS12**, and (e) **GS13** dyes.

Grätzel's group synthesized a panchromatic dye (black dye), **N749** (Figure 1.4a), using a tridentate terpyridine derivative ligand and three thiocyanato ligands [28]. The development of such a panchromatic dye is the ideal approach under the conventional strategy. The absorption spectrum of the sensitizer was extended by the introduction of three thiocyanato ligands that shift the ruthenium(II) t_{2g} orbitals upward. The LUMO level was kept at a more negative potential than the conduction band of TiO_2 , and the HOMO was located at a sufficiently positive potential relative to the redox potential of the reductant (i.e. iodide). Recently, Segawa and coworkers developed a phosphine-coordinated Ru-complex sensitizer, **DX1** (Figure 1.4b) [29]. Their approach to extending the absorption of the dye is unconventional in that it involves a spin-forbidden transition. Figure 1.5a shows the absorption and emission spectra as functions of the energy diagrams of **DX1**, along with the spectrum of a black dye. In the case of **DX1**, the singlet-triplet transition is emphasized clearly, and this extension of the light-absorption spectrum improved the power conversion efficiency in a DSSC system.

DX1 and its derivatives have been investigated in a DSP for H_2 evolution [13]. Four phosphine-coordinated Ru complexes (Figure 1.4b–e) were synthesized; their energy diagrams are shown in Figure 1.5b. In all cases, the LUMO level was sufficiently negative for excited-electron injection into the conduction band of TiO_2 . These four panchromatic photosensitizers were applied to the photocatalytic H_2 -evolution reaction on Pt-modified TiO_2 , where triethanolamine (TEOA) was used as a sacrificial electron donor. **GS12** showed the highest H_2 -evolution activity, and the apparent quantum yield (AQY) for H_2 evolution under irradiation by a 400 W Hg lamp reached 5.16%. This value is 5.5 times greater than that of **N719** under the same conditions. The activity increased in the order **GS12** > **GS11** > **DX1** > **GS13**, and this trend obviously reflects the LUMO energy level. These results indicate that

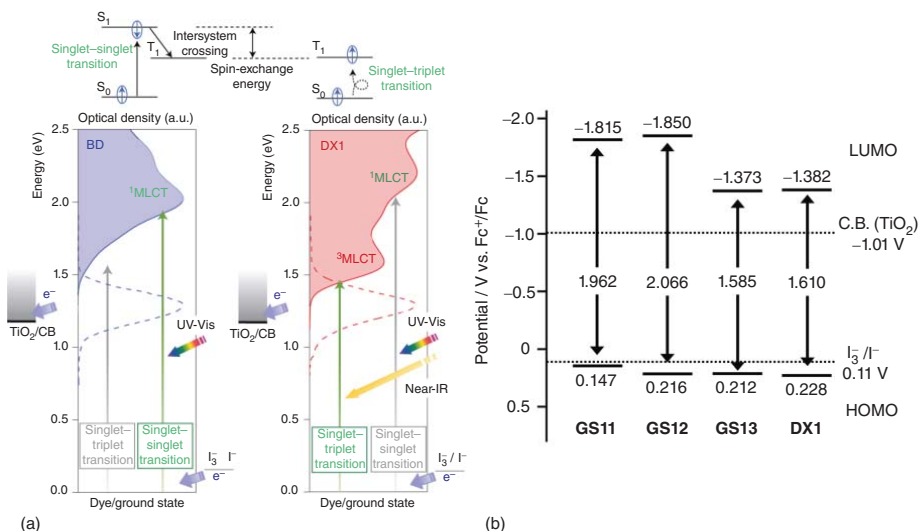


Figure 1.5 (a) Energy diagram of the components and the device performance of the sensitizers. Absorption (solid line) and emission (dashed line) spectra vs. the energy diagrams of BD (black dye, **N749**, left) and **DX1** (right). In the singlet-to-singlet transition, the electron transition from the S_0 to the T_1 excited states causes energy loss via spin-exchange energy (top). Source: Reproduced with permission from Kinoshita et al. [29]; © 2013, Springer Nature. (b) Schematic energy levels of **GS11**, **GS12**, **GS13**, and **DX1**. Source: Adapted with permission from Swetha et al. [13]; © 2015, American Chemical Society.

the DSP performance for the H₂-evolution reaction can be enhanced by negatively shifting the oxidation potential of the dye in the excited state. The use of a panchromatic dye in a dye-sensitized H₂-evolution system improved the photocatalytic activity, and an investigation of the **DX1** derivatives revealed that regulation of the LUMO energy level is an important consideration in the molecular design of sensitizers.

1.2.2 Enhancement of the Absorption Coefficient of Dyes

Increasing the molar extinction coefficient of dyes is a straightforward method of increasing the solar energy conversion efficiency in a dye-sensitization system. Making the π -chromophore more rigid is a common tactic to increase the molar extinction coefficient. Rigid molecules can suppress the rotational disorder and enhance the delocalization capacity of π -electrons [30]. At the same time, however, increasing the rigidity of molecules promotes aggregation, and undesirable aggregation often adversely affects the energy conversion performance via, e.g. competitive nonradiative quenching and a hypsochromic shift of the dye [31]. As an alternative approach to enhancing the molar extinction coefficient, Ning et al. proposed incorporating an additional electron donor unit into the dye to form a starburst 2D- π -A conjugate [32]. This approach is promising for increasing light-harvesting performance; however, the number of reported starburst 2D- π -A structures is limited because of their complicated synthetic pathways. To address this problem, organoboron complexes have been investigated as relatively small and simple π -chromophore units.

The approach of incorporating organoboron complexes has been applied to a phenothiazine-based dye [30]. Phenothiazine (Figure 1.6a) is one of the most extensively studied electron-donor components and exhibits strong electron-donating character because of its heterocyclic structure containing S and N [33]. Because of its strong electron-donating ability, an early phenothiazine-based dye achieved a solar-energy-to-electricity conversion efficiency comparable to that of **N3** dye [34]. Further improving the efficiency of the phenothiazine-based dye system is difficult because of its low molar extinction coefficient. Given this background, the incorporation of organoboron complexes into phenothiazine-based dyes is attractive. In particular, 4,4-difluoro-4-bora-3a,4a-diaza-s-indacene (BODIPY, Figure 1.6b) dyes exhibit high molar absorptivity and sharp fluorescence peaks, along with a high QY [35]. A series of BODIPY derivatives, pyridomethene-BF₂ complexes (Figure 1.6c), exhibit a very large extinction coefficient ($5 \times 10^4 \leq \epsilon \leq 1.4 \times 10^5 \text{ M}^{-1} \text{ cm}^{-1}$). Among the emission quantum efficiencies of the derivatives, the highest was similar to that of **N719** [30]. To further improve BODIPY-sensitized systems, Erten-Ela et al. developed a dibenzo-BODIPY dye (Figure 1.6d) using a conventional strategy, with the objective of extending the π -conjugation and enabling longer-wavelength absorption [36]. The dibenzo-BODIPY was combined with phenothiazine (Figure 1.6e), and the absorption reached the near-infrared (NIR) region. The efficiency of BODIPY-sensitized solar cell systems eventually overtook that of **N719** systems [36]. The dibenzo-BODIPY and phenothiazine combined dye has

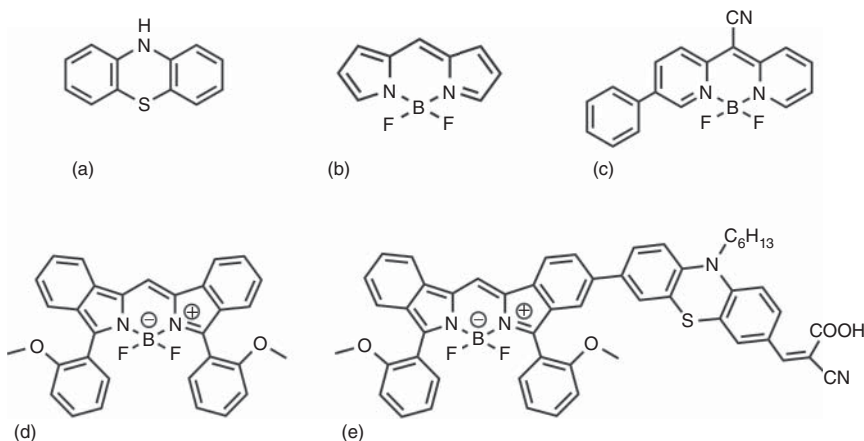


Figure 1.6 Molecular structures of (a) phenothiazine, (b) BODIPY, (c) the parent pyridomethene- BF_2 complex, (d) dibenzo-BODIPY dye, and (e) a phenothiazine dye with dibenzo-BODIPY incorporated.

been applied to the H_2 -evolution reaction on Pt-modified hierarchical porous TiO_2 , where ascorbic acid (AA) was used as a sacrificial electron donor [37]. The turnover number of the dye for H_2 evolution reached 11,100 under visible-light irradiation ($\lambda > 400 \text{ nm}$) at an intensity of 100 mW cm^{-2} . The organoboron-phenothiazine dye improved the visible-light absorption performance and demonstrated high H_2 evolution activity in metal-free organic dyes. That is, a binary electron donor system comprising a small and simple π -chromophore unit incorporated into an electron-donor building block functioned well as a dye-sensitized photocatalyst system.

1.2.3 Molecular Design for Efficient Excited-Charge-Carrier Separation and Injection

Efficient charge-carrier separation and injection into a semiconductor strongly affects the efficiency of a dye-sensitized system. As previously described, the visible-light absorption of dyes relies predominantly on a charge-transfer (CT) transition between donor/acceptor units. The donor unit should be physically separated from the semiconductor to suppress back electron transfer from the semiconductor and to facilitate the reaction with a reductant in the reaction solution. The acceptor unit should be physically close to the semiconductor to enable the immediate transfer of an excited electron into the semiconductor. To improve the energy conversion efficiency through the molecular design of dyes, tracing the history of the development of sensitizer molecules and understanding the roles of the building blocks of dye molecules would be beneficial. Here, a triphenylamine-based dye, which is one of the most studied organic photosensitizers, is used as an example and the history of the development of dyes is described.

Triphenylamine has been studied extensively as an electron-donor unit since the early 2000s [20]. In the earliest study of triphenylamine as a donor unit,

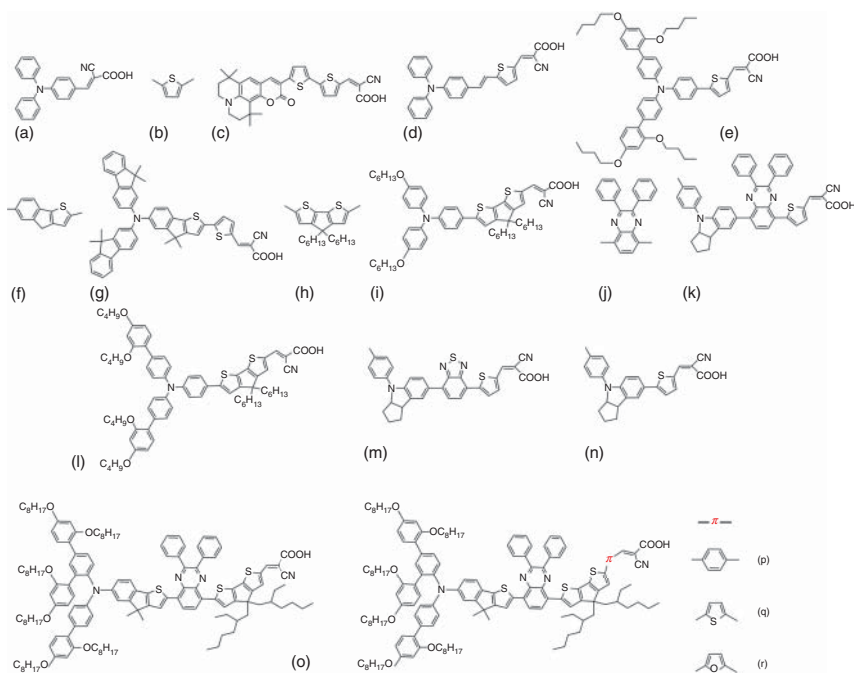


Figure 1.7 Molecular structures of (a) one of the earliest developed triphenylamine-based dyes, (b) the thiophene moiety, (c) a thiophene-bridged coumarin dye (**NKK-2677**), (d) dye **D5**, (e) dye **D35**, (f) the indeno[1,2-*b*]thiophene moiety, (g) an indeno[1,2-*b*]thiophene-bridged dye (**JK-225**), (h) the cyclopentadithiophene moiety, (i) a cyclopentadithiophene-bridged dye (**C218**), (j) a 2,3-diphenylquinoxaline unit, (k) a 2,3-diphenylquinoxaline-incorporated dye (**IQ4**), (l) **LEG4**, (m) **WS-2**, (n) **LS-1**, (o) **S5**, (p) **SD1**, (q) **SD2**, and (r) **SD3**.

dyes consisting of carboxylic and cyano moieties as electron-donor and -acceptor groups, respectively, were developed (Figure 1.7a) [18]. Because the carbon–carbon double-bonded π -bridge in these dyes is problematic in terms of the synthesis and stability of the molecule, a thiophene moiety (Figure 1.7b) was incorporated as a new π -conjugation unit to address these problems in a coumarin dye (Figure 1.7c) [38]. Combining these moieties, Hadberg et al. developed one of the simplest-structured triphenylamine-based dyes, named **D5** dye (Figure 1.7d), which gave an energy conversion efficiency comparable to that of **N719** [39]. The para-position of the triphenylamine unit was subsequently substituted to increase the electron-donating character (Figure 1.7e) [40]. Indeno[1,2-*b*]thiophene (Figure 1.7f,g) [41] and cyclopentadithiophene (Figure 1.7h,i) [42] units were used to expand the π -conjugation system. A 2,3-diphenylquinoxaline unit (Figure 1.7j,k) [43] was introduced not only as an acceptor unit but also as a building block to limit intermolecular aggregation. The use of these good building blocks (electron donor, electron acceptor, and π -conjugation units) led to the development of a triphenylamine-based D– π –A-structured dye, **LEG4** (Figure 1.7l), and its derivatives [44].

Further improvement of D- π -A-structured dyes was realized through a new molecular design: the donor-acceptor- π -acceptor (D-A- π -A) structure [45]. To explain the effects of electron-acceptor insertion between the electron-donor and π -bridge, we here discuss two dyes (**WS-2** and **LS-1**, Figure 1.7m,n, respectively) as examples. They possess an indoline-based electron donor, a thiényl π -linker, and a cyanoacrylic acid electron acceptor. The D-A- π -A dye **WS-2** has benzothiadiazole (BTD) as an additional electron acceptor. The incorporation of an electron-acceptor unit between the electron-donor and π -conjugation units influences the electronic state of the molecule, as confirmed by a density functional theory simulation of the BTD-inserted D-A- π -A dye **WS-2**. The HOMO and LUMO distributions both clearly overlap the orbitals of the BTD unit, which is beneficial for the electron transition. Comparing these two sensitizers reveals four advantages of the **WS-2** dye: (i) strong light-harvesting ability because of the bathochromic shift of the absorption associated with CT, (ii) the appearance of an additional absorption band attributed to a secondary frontier orbital transition, (iii) suppression of the hypsochromic shift that accompanies adsorption onto a TiO_2 film, and (iv) improvement of the stability for light absorption because of the decrease in the LUMO level. The substantial improvement of the light-absorption capability as a result of the formation of the D-A- π -A structure contributed to a high power conversion efficiency of 9.04% [46].

This new strategy led to the development of a derivative of the **LEG4** dye (**S5**, Figure 1.7o) [47], along with dyes with a different π -bridge, **SD1-3** (Figure 1.7p-r) [21]. The SD dye series was used in both DSSC and H_2 -evolution DSP systems. Interestingly, the performance of the dyes was varied dramatically in the different systems. In the DSSC system, in which $[\text{Co}(\text{bpy})_3]^{3+/2+}$ was used as an electron mediator, **SD1** exhibited the highest power conversion efficiency and the order of efficiency was **SD1** > **SD3** > **SD2**. These results are attributed to **SD1** reducing charge recombination as a result of its large torsional angle and large driving force for regenerating the dye ground state. In the DSP system, by contrast, **SD2** demonstrated the highest H_2 -evolution activity on Pt/TiO_2 , where AA was used as an electron donor. Spectroscopic and photoelectrochemical studies revealed that the fastest electron injection into Pt/TiO_2 and the lowest charge-carrier transfer resistance were achieved in the **SD2** system. The highest performance of **SD2** toward H_2 evolution is likely a consequence of its good electron transfer and electron-hole separation process. **SD1**, which exhibited the highest efficiency in the DSSC system, exhibited the lowest activity toward the H_2 -evolution photocatalytic reaction. This different tendency is attributed to differences in the reaction conditions. The electrons injected into TiO_2 migrate to the electrode under an electrical bias in a DSSC system and are consumed by the surface H_2 -evolution reaction in a DSP system. The different reaction solutions (organic solvent vs. aqueous solution) can render the dye hydrophilic or hydrophobic. The electron donor, which is the electron mediator and sacrificial reductant in each system, should influence the efficiency of the oxidation reaction. The importance of the hydrophilicity and the reaction with a reductant will be discussed in the next section.

1.2.4 Molecular Design for Facilitating the Regeneration of the Ground State

Accelerating the reduction reaction of a sensitizer in the oxidized state to regenerate the ground state is important for improving the stability of a dye because the oxidized state of a dye is decomposed via light absorption of the oxidized state itself. To investigate the influence of the electron-donor unit structure, in which the LUMO is distributed, for the regeneration reaction of the sensitizer, Bartolini et al. carried out H₂-evolution reactions using triphenylamine-based D-A-π-A dyes with and without functionalization by bulky hydrophilic substituents (Figure 1.8) [22]. **Dye1** has no special substituents on the terminal of triphenylamine, whereas **Dye2** has four bis(ethylene glycol) monomethyl ether (BEG) chains. The BEG chains improve the hydrophilicity of the sensitizer and also behave as a steric, bulky moiety. The H₂-evolution reactions were conducted in aqueous solutions containing TEOA or AA as a sacrificial electron donor (SED), and the activities were exactly opposite depending on the SED used. When TEOA was used as the SED, the H₂-evolution activity of the **Dye1** system was twofold greater than that of the **Dye2** system.

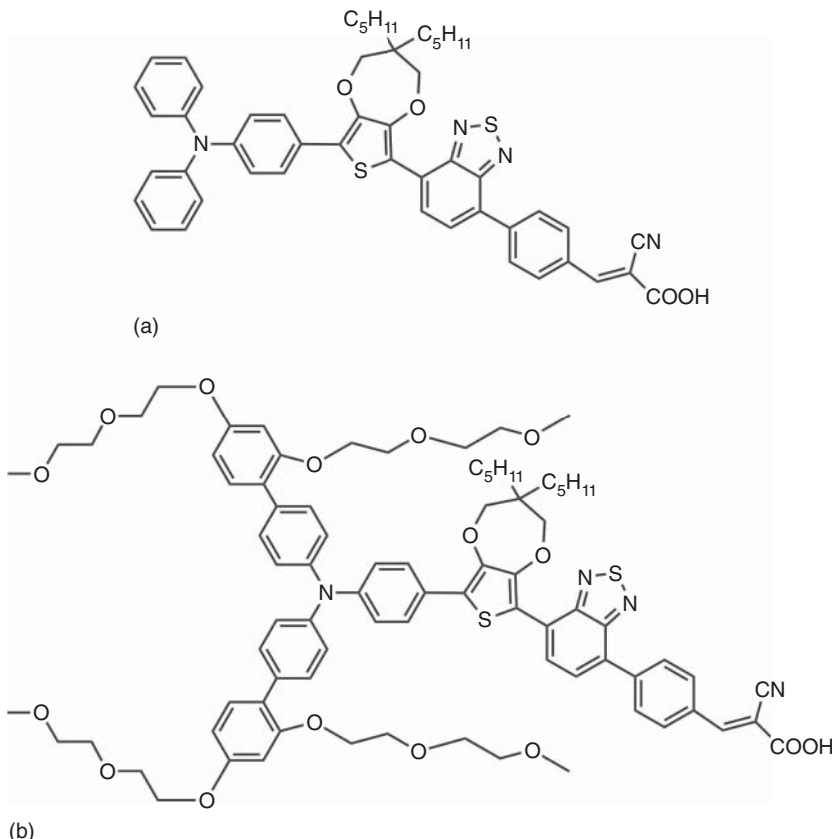


Figure 1.8 Molecular structures of (a) **Dye1** and (b) **Dye2**.

By contrast, when AA was used as the SED, the **Dye2** system exhibited twofold greater activity than the **Dye1** system. The amount of H₂ evolved when AA was used was eighteen-fold greater than that when aqueous TEOA solution was used. The large influence of the SEDs and the hydrophilic substituent on the activities can be explained in terms of the interaction between them. In the TEOA system, because no noticeable interaction occurs between the BEG chains and TEOA, such a steric bulky substituent would inhibit the access of TEOA to the electron-donor unit (triphenylamine). The suppression effect dramatically decreases the efficiency for regenerating the dye ground state, leading to very low activity for H₂ evolution. In the AA system, however, BEG chains would strongly interact with the highly polar SED, thereby accelerating the regeneration of the sensitizer ground state. That is, the hydrophilic substituent suppresses the oxidation reaction of TEOA but promotes that of AA. Therefore, a large difference in activity between the two SEDs was observed in the **Dye2** system.

The effects of hydrophobicity and hydrophilicity have also been studied in other sensitizer systems. In a carbazole-based dye system whose electron-donor unit is similar to triphenylamine, long alkoxy chains were found to improve the hydrophobicity of the dye and to increase the H₂-evolution activity in an aqueous TEOA solution [48]. Enhancing the hydrophobicity suppressed undesirable charge recombination and contributed to an improvement of the photocatalytic activity. Modification of phenothiazine with glucose through a triazole ring unit improved the hydrophilicity, thereby improving the photocatalytic H₂-evolution performance when TEOA was used as an electron donor [49]. The improvement of the activity was due to acceleration of the reaction with a reductant in aqueous solution and to suppression of intermolecular quenching, the latter of which was induced by insertion of a sterically bulky moiety. The effect of wetness around dye molecules on the excited electron-transfer process was investigated using Ru complexes [50]. Protons in water adsorbed onto the substrate oxide (TiO₂) tended to assemble around the dye molecules under dry conditions but not under wet conditions, causing instability in the oxidized form of the photosensitizer generated by electron injection. Destabilization of the oxidized dye decreased the efficiency of the electron injection.

1.2.5 Improving Stability by Forming a Strong Connection Between a Dye and a Semiconductor

A dye excited by light absorption can be desorbed from the substrate surface and/or decomposed because of its instability. The desorption and decomposition result in deactivation of the dye-sensitized system. As described in the Introduction, a dye sensitizer follows a cycle involving photoexcitation, electron injection, and regeneration. Fast regeneration of the ground state should improve the efficiency because deactivation is suppressed, as discussed in Section 1.2.4. Similarly, the excited state, which is more unstable than the oxidized form, needs to be transformed immediately to the oxidized state to improve the stability of the system; that is, fast electron injection into a semiconductor will improve the durability of a

dye-sensitized system. Robust adsorption of a dye onto a semiconductor suppresses desorption of the dye and simultaneously accelerates the electron injection via strong interaction between the sensitizer and the semiconductor. The electron-injection rate strongly depends on the electronic coupling between the density of states in the semiconductor and the electron-donating orbital of the sensitizer. In the **N3-TiO₂** system, ultrafast electron injection was observed (~50 fs) because of the relatively high density of states of TiO₂ and favorable coupling with the electron-donating orbital (the π^* orbital of the carboxyl-anchoring group of the substituted bipyridine of **N3**) [51]. Therefore, strong bonding between a dye and a semiconductor is a promising way to improve the longevity of a dye-sensitized system from the viewpoint of not only desorption but also decomposition.

A representative anchoring group used in DSSCs is the carboxyl moiety; however, the carboxyl moiety is prone to desorption in aqueous solution. A phosphonic acid moiety improves the stability in weakly acidic conditions, whereas most carboxylate-anchoring groups are desorbed at pH \approx 6 [52]. Because metal complex dyes, especially those based on Ru(II) trisdiimine complexes, enable chemical functionalization with various ligands, the effect of the number of anchoring groups on the dyes' desorption stability and DSSC performance has been studied [52]. However, introducing multiple anchoring groups into an organic molecular dye is synthetically difficult, although the literature contains numerous reports related to multiple branching and anchoring metal-free molecular dyes [53].

A calix[4]arene-based organic dye, which is easy to synthesize and has multiple anchoring groups, was developed (Figure 1.9a) [54]. Calix[n]arene ([n]: number of units) is a ring oligomer constructed by several units that consist of methylene-substituted phenols. The four phenol units are combined with a π -conjugation unit and constitute an electron-acceptor unit. Therefore, the calix[4]arene-based dye has four D- π -A structures in one molecule. All the calix[4]arene-based dyes show a cone conformation (Figure 1.9c) with an electron-acceptor unit at the top and anchoring groups at the bottom of the cone. When this sensitizer was used as a DSSC device, the system operated for 500 hours with no degradation in performance and showed high stability under light irradiation. A calix[4]arene derivative, **HO-TPA**, was effective for DSP for the H₂-evolution and CO₂-reduction reactions (Figure 1.9b) [55]. Stable H₂-evolution activity was observed for 75 hours. The **HO-TPA** dye has calix[4]arene and triphenylamine moieties as electron-accepting and -donating units, respectively. The donor-acceptor units are conjugated by an oligothiophene moiety. This sensitizer has four -OH anchoring groups at the calix[4]arene ring, which is the conical top, and the unique structure is beneficial for suppressing dye aggregation and forming strong bonds with the substrate surface.

1.2.6 New Insights Based on the Light Harvesting of a Dye-sensitized Photocatalyst System

Dyes have been developed not only through the traditional strategy (as described in Section 1.2.1) but also through unconventional approaches based on a novel concept. To suppress dye aggregation, Manfredi et al. introduced a coadsorbent

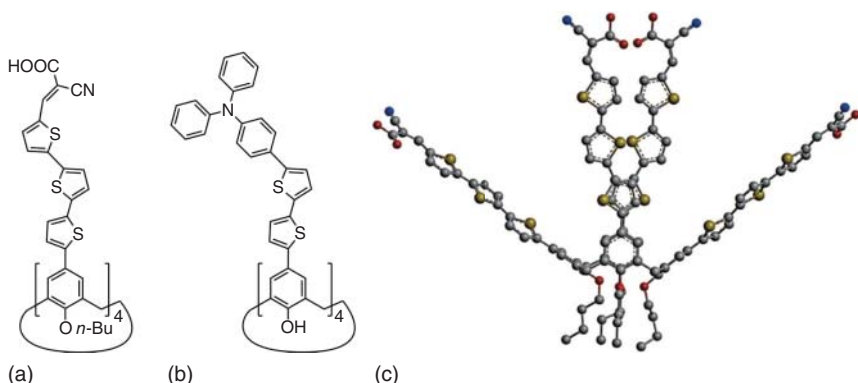


Figure 1.9 Molecular structures of (a) **Calix-3** and (b) **HO-TPA**. (c) The optimized geometry of the **Calix-3** dye was mimicked through molecular modeling with the GAUSSIAN 03 package. Source: Reproduced with permission from Tan et al. [54]; © 2015, John Wiley & Sons, Inc.

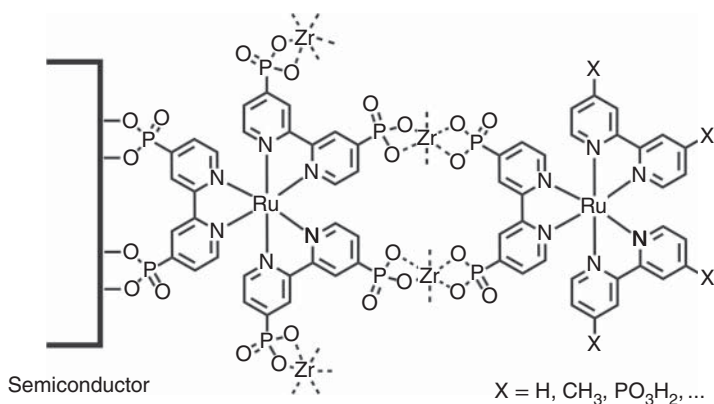


Figure 1.10 Schematic of the “layer-by-layer” assembly.

that does not function as a light absorber [56]. The H₂-evolution photocatalytic activity was doubled when the coadsorbent was adopted because it suppressed undesirable interaction among dye molecules. A direct electronic transition induced by visible light from a simple, small dye (an azoquinoline carboxylic acid) into a semiconductor (ZnO) was proposed [57]. This transition was enabled by the formation of a novel electronic state because of strong coupling between the dye and ZnO, and the transition could be used for a visible-light H₂-evolution reaction.

To effectively utilize the limited semiconductor surface, Mallouk and coworkers used a “layer-by-layer” (LBL) assembly approach [58]. This approach introduces multiple redox-active and/or chromophores onto a metal-oxide surface by forming phosphonate/Zr⁴⁺ coordination linkages (Figure 1.10) [59]. A bilayer assembly composed of two layers of Ru(II) complexes exhibited an approximately twofold increase in absorbance compared with a monolayer complex film. The assembly